Research Article | Vol. 11, No. 2 / 1 February 2020 / Biomedical Optics Express 850
Biomedical Optics EXPRESS

Analytical solution of a personalized intraocular lens design for the correction of spherical aberration and coma of a pseudophakic eye

Bruno Chassagne[1,*] and Lionel Canioni[2]

[1]*ALPhANOV Centre Technologique Optique et Lasers, Institut d'Optique d'Aquitaine, 33400 Talence, France*
[2]*Université de Bordeaux, CNRS, CEA, CELIA, UMR 5107, F-33405 Talence, France*
[*]*bruno.chassagne@alphanov.com*

Abstract: This manuscript reports on a closed-form solution determining the personalized required shape of a new intraocular lens able to remove spherical aberration and coma of a pseudophakic eye. The proposed analytical method, within the framework of the Seidel theory of third-order optical aberrations, considers corneal conicities, fourth-order aspheric surface of the intraocular optics, pupil-shift effect and ocular kappa angle.

1. Introduction

Pseudophakia, or pseudophakic eye, corresponds to an eye in which the natural crystalline lens is replaced with an intraocular lens (IOL) after cataract surgery. In the case of a monofocal lens, the objective is obvisouly to optimize the pseudophakic eye for far vision and the evaluation of the IOL power has been an important area of study [1,2].

Concerning optical aberrations handling, two main approaches of IOL are used. In the first one, the IOL design is calculated with a sufficient negative spherical aberration (SA) in order to balance the positive corneal SA and then reduce optical aberrations of the whole pseudophakic eye [3,4–6,7]. As an example, this is the case of the Tecnis^{TM} Z9000 IOL [8] and the Invent ZO from Carl Zeiss [9]. Those IOLs are often called aberration-correcting IOLs and the design of their anterior or posterior surface usually includes conic constant and high-order aspheric coefficients (up to the 14th power). In the second one, for some pathologies, rather than trying to correct for the positive corneal SA, the IOL is designed without any inherent SA to avoid introducing more aberration to the pseudophakic eye. These IOLs are often referred as aberration-free IOLs [10,11]. The design of their form is usually bi-convex lens with at least one conic surface. For example, the product SofPort AO from Bausch & Lomb is one of them [11]. It is worth remembering, the higher optical degradation of the retinal image in the presence of decentration and tilt after capsular bag implantation is obtain with high-order aspherical IOL. Lenses whose geometrical design is less complex [12–14] exhibit less optical degradation to misalignment.

In this study we only consider the design of monofocal aberration-correcting IOLs for far vision. Moreover, we did not evaluate the effect of optimization of SA on depth of focus and ignored the neuroadaptive response.

It has been shown [11] that for a mean decentration limited to ± 0.3 mm, the aberration-correcting IOL concept provides very good imaging quality at the specific spatial frequency of 30 cycles/degree, corresponding to a visual acuity of 20 / 20. Several clinical studies showed that the mean absolute values for tilt and decentration, after cataract surgery, are respectively $\sim 2.5°$ and 0.3 mm [11,14–16]. Whereas, if perfect alignment within this tolerance cannot be guaranteed in cases with persisting pathologies, aberration-free IOLs are the only choice. Indeed, this is an acceptable compromise between acceptable retinal imaging and a design robust to decentration and tilt [11].

#382162 https://doi.org/10.1364/BOE.382162
Journal © 2020 Received 1 Nov 2019; revised 19 Dec 2019; accepted 28 Dec 2019; published 14 Jan 2020

Biomedical Optics EXPRESS

Using aspheric surfaces provides for the optical designer, the ability for reducing optical aberrations not only on-axis but also off-axis [3]. It is known that the foveal eccentric position, located on the temporal side, results in angular differences between the visual axis (*i. e.* the line of sight joining the fovea with the center of the pupil) with the optical axis of the eye, of ~ 5° [17]. Due to this physiologic ocular tilt, the eye experiences corneal coma and oblique astigmatism. An IOL design was early proposed by Smith *et al.* to correct peripheral powers errors and astigmatism of eyes [18] and Tabernero *et al.* also proposed an optimized aberration-correcting IOL able to correct corneal SA and lateral off-axis coma with the use of high-order aspheric surfaces [17]. In this former publication, the authors used Zemax optical ray tracing software [19] to optimize their IOL. Nevertheless, they started their study with a simple analytical Seidel aberration formalism to determine the best IOL shape needed for the corneal coma correction. This algebraic optical formalism considers only bi-convex IOLs. It does not take into account the corneal conicity of the eye and neglect the separation between the cornea and the IOL final location. By doing so, it is omitting the extra-coma contribution generated by the corneal SA when pupil-shift law is applied. Despite of these approximations, this former analytical formalism gives good results for high power IOLs [17].

Currently, even if an experimental study showed that IOL with negative SA are capable to produce an almost complete compensation of horizontal coma [20], most of available aberration-correcting IOLs design compensate for average spherical aberration only, and for on-axis performance, analytical model optimizing monofocal IOL can be found in the literature [21]. In this article, we present an analytical solution determining the required shape for a new aspheric IOL to minimize global on- and off-axis aberrations (SA and coma) of a pseudophakic eye. This analytical model (Microsoft Excel sheet available in the supplemental document of this article), that takes into account for the first time to our knowledge, corneal conicities, 4th-order aspheric surface, pupil-shift effect and ocular kappa angle, enables the design of custom IOL for an individual compensation of corneal aberrations. It is in good agreement with results given by Zemax simulation and the performances of the resulting calculated new IOL compare well with those obtained with commercial IOLs.

2. Model

A classical analytical form of aspheric surface is defined by the following sag equation:

$$z = \frac{c_u h^2}{1 + \sqrt{1 - (1+Q)c_u{}^2 h^2}} + \varepsilon_4 h^4 + \varepsilon_6 h^6 + \ldots \tag{1}$$

Where h is the radial coordinate, c_u is the base curvature at the vertex, Q is the conic coefficient and (ε_i) are the higher order aspheric terms. In the framework of the Seidel aberration formalism, among the higher order aspheric terms, only ε_4 contributes to the amount of aberration. It is known that the ε_4 term can be made zero with a series development limited to order 4, and hence omitted if the value of the conicity Q is changed to $Q' = Q + 8\varepsilon_4/c_u{}^3$ [4,5]. This means that a 4^{th}-order aspheric surface can be mathematically seen and defined as a pure conic surface and vice versa. For an IOL with a pure 4^{th}-order aspheric surface, given by Eq. (2), we can then expect to be able to have simultaneously very good optical correction of the SA and coma for the pseudophakic eye (advantage given by the 4^{th}-order aspheric term ε_4) with a good sensitivity to misalignment (advantage given by the "equivalent pure conic term" $8\varepsilon_4/c_u{}^3$) than those of IOLs that belong to the "aberration corrected" concept. Finally, we also specify that the benefits of the aspheric over the conic surface design have been quantitatively evaluated by Barbero *et al.*, that showed that using aspheric profiles allows ~ 12% improvement of the optical quality with

Biomedical Optics EXPRESS

respect of using conic surfaces [3].

$$z = \frac{c_u h^2}{1 + \sqrt{1 - c_u^2 h^2}} + \varepsilon_4 h^4 = \frac{c_u h^2}{1 + \sqrt{1 - (1 + Q')c_u{}^2 h^2}} \tag{2}$$

In the proposed following model, we considered the same aspherization of the anterior surface of the IOL as the aspherization of the posterior one. This is equivalent for the calculated IOL, to consider a 4th-order aspheric coefficient ε_4 for the front surface and -ε_4 for the back one (see Fig. 1). Obviously, aspherizing just one surface (anterior or posterior) of the IOL is also possible, and the formulas of the following model can be easily calculated. The overall optical performances of the pseudophakic eye in this case are lower than in the symmetric case, in particular for low power IOLs.

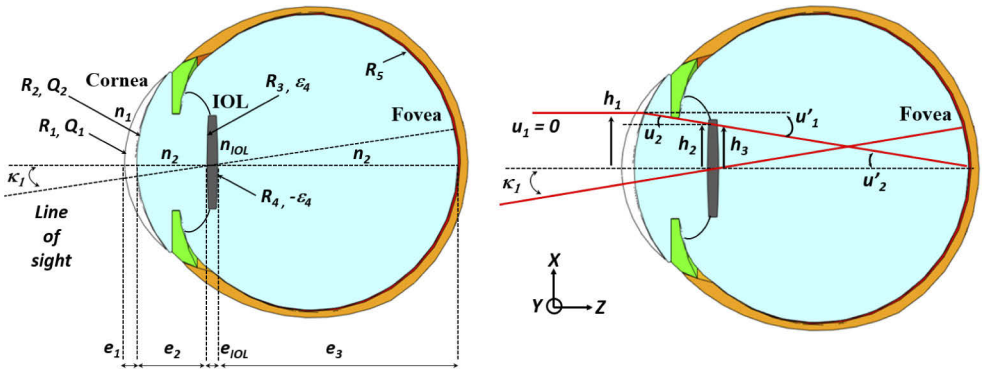

Fig. 1. Schematic description of a pseudophakic eye (left) and definition of geometrical parameters for the paraxial principal and marginal rays (right).

The geometrical parameters of the pseudophakic eye, including an IOL with a pure 4th-order aspheric surface, and paraxial data that will be used in the model, are illustrated in Fig. 1.

For the calculations we used the classical and physiologically accurate LBME model of the eye [22], including conic corneal surfaces, in which the natural crystalline lens is replaced by the IOL. Table 1 shows the corneal properties used for the simulation at a wavelength of 555 nm, corresponding, for photopic vision, to the maximum of spectral sensitivity of the eye. In the following, all calculations were done for a monochromatic light of 555 nm. Obviously, depending on the biometry of each patient's eye, those values are set as parameters in the presented model and can be easily changed.

Table 1. LBME model of corneal values and IOL's parameters used in the simulation

Surface	Radius (mm)	Thickness (mm)	Conic constant	4th order aspheric term	n (λ=0.55 µm)
Anterior Cornea	$R_1 = 7.77$	$e_1 = 0.5$	$Q_1 = -0.18$	0	$n_1 = 1.376$
Posterior Cornea	$R_2 = 6.4$	Aqueous depth e_2	$Q_2 = -0.6$	0	$n_2 = 1.336$
Anterior IOL	R_3	e_{IOL}	0	ε_4	n_{IOL}
Posterior IOL	R_4		0	$-\varepsilon_4$	
Vitreous	-	Vitrous chamber depth e_3	-	-	$n_2 = 1.336$
Retina (R_5)	$R_5 = -12$	-	0	-	-

Biomedical Optics EXPRESS

Expressions for the primary aberrations of lenses have been given by a number of authors and we modified their formulation given in Ref. [23], in order to take into account conicity and asphericity of the different dioptres, to evaluate them for the pseudophakic eye. Useful paraxial parameters used to calculate those Seidel sums such as height, angle of the principal ray, ocular physiologic kappa angle κ_1, Lagrange optical invariant H, and Coddington shape factor X, are expressed in Table 2. In order to explore the dependence of aberrations on lens shape, the Coddington factor is helpful [23] and we recall that a change in the shape factor X of a lens leads to different changes of the curvatures of its surfaces, as the power of the lens remains unchanged.

Table 2. Expression of parameters (see text and Fig. 1 for details)

Parameters	Expression	Parameters	Expression
P_C Corneal power	$\frac{n_1-1}{R_1}-\frac{n_1-n_2}{R_2}$	H Lagrange invariant	$h_1\kappa_1$ (κ_1 : ocular physiologic kappa angle, see Fig. 1)
$f_{Canterior}$ Anterior corneal focal length	$\frac{n_1}{n_1-1}R_1$	h_2	$h_1\left(1-\frac{e_1}{f_{Canterior}}-\frac{e_2}{n_2}P_C\right)$
X_C	$(\frac{n_1-1}{R_1}+\frac{n_1-n_2}{R_2})\frac{1}{P_C}$	h_3	$h_2-\frac{e_{IOL}}{n_{IOL}}\left[\frac{h_2}{2}P_{IOL}(X_{IOL}+1)+h_1P_C\right]$
Y_C	1	h_{mean}	$\frac{h_2+h_3}{2}$
P_{IOL} IOL power	$(n_{IOL}-n_2)(\frac{1}{R_3}-\frac{1}{R_4})$	$u'_1=u_2$	$h_1\frac{P_C}{n_2}$
X_{IOL}	$\frac{(n_{IOL}-n_2)}{P_{IOL}}(\frac{1}{R_3}+\frac{1}{R_4})$	u'_2	$\frac{h_{mean}P_{IOL}+h_1P_C}{n_2}$

2.1. Corneal aberrations

In the formalism of [23], primary Seidel aberrations are written as polynomial linear combination of power of the shape factor X and position factor Y. For cornea, those two former values X_C and Y_C (where the subscript C is for Cornea) are specified in Table 2. In particular, for far vision, $u_1=0$ (see Fig. 1) then $Y_C=1$ [23]. Assuming cornea as a thin lens and the stop position located on it, the corneal SA is given by:

$$S_I^C=\frac{1}{8}h_1^4P_C^3\left[a_1^CX_C^3+a_2^CY_C^3+a_3^CX_C^2Y_C+a_4^CX_CY_C^2+a_5^CX_C^2+a_6^CY_C^2+a_7^CX_CY_C+a_8^CX_C+a_9^CY_C+a_{10}^C\right]+(n_1-1)\frac{h_1^4}{{R_1}^3}Q_1+(n_2-n_1)\frac{h_1^4}{{R_2}^3}Q_2 \quad (3)$$

where the $a_i{}^C$ factors are known functions of the refractive indexes (n_1, n_2) tabulated in [23] and where we added the conicity of the cornea, represented by the two last terms. The $a_i{}^C$ factors are described in Appendix A.

In the same way, for primary coma, we have for cornea [23]:

$$S_{II}^C=\frac{1}{4}h_1^2P_C^2H\left[p_1^CX_C^2+p_2^CY_C^2+p_3^CX_CY_C+p_4^CX_C+p_5^CY_C+p_6^C\right]+(n_2-n_1)(\frac{e_1\kappa_1}{n_1})\frac{h_1^3}{{R_2}^3}Q_2 \quad (4)$$

As again the $p_i{}^C$ factors for coma's coefficients are tabulated as functions of refractive indexes and given in Appendix B.

It is now important to specify that the pupil location of the eye will be close to the IOL. In fact, we will suppose that the diameter of the anterior surface of the IOL represents the stop of the system. It means that we have to calculate the aberration of the cornea due to this stop-shift given by the distance (e_1+e_2) (see Fig. 1). Then, the amount of corneal aberrations calculated in

Biomedical Optics EXPRESS

the plane of the anterior surface of the IOL, is given by:

$$(S_I^C)^* = S_I^C \tag{5}$$

$$(S_{II}^C)^* = S_{II}^C + S_I^C \times \frac{\kappa_1}{h_1 P_C} \times [1 - \frac{1}{1 - \frac{(e_2+e_1)P_C}{n_2}}] \tag{6}$$

The asterisk indicates aberrations values modified by the stop-shift when the considered pupil of the system is no longer on the cornea but is in the IOL plane. We note the extra-coma contribution, generated by the corneal SA (see Eq. (6)), when this pupil-shift law is applied. Finally, Table 3 evaluates those former corneal aberrations as a function of the pupil size and the field of view, for the numerical values of the LBME model given in Table 1 and for coefficients of Appendixes A and B. Those formulas, that will be used later, can be of practical interest to keep in mind the order of magnitude of each corneal aberration.

Table 3. Numerical evaluation ($\lambda = 555$ nm) for LBME model of corneal aberrations as a function of pupil size (h_1) and angular field (ocular kappa angle κ_1) due to off-axis fovea

Parameters	Expression	Parameters	Expression
P_C	42.1 D	${S_I}^C$	$\sim 3.16\times10^{-4}\times{h_1}^4$
X_C	1.297	${S_{II}}^C$	$\sim 0.003\times\kappa_1\times{h_1}^3$
		$({S_{II}}^C)^*$	$\kappa_1 \times {h_1}^3 \left[0.003 + 0.00751 \left(1 - \frac{1}{1-0.0315(e_2+0.5)}\right)\right]$

As an example, for a pupil size of 6-mm ($h_1 = 3$ mm), our Seidel formalism (Table 3) gives a corneal SA of ${S_I}^C \sim 0.026$ mm. One can compare it to the well-known Zernike formulation. In terms of Zernike polynomial formalism and for a 6-mm aperture diameter, experimental reported results gave a root-mean-squared (RMS) Z_4-value for corneal SA of (0.27 ± 0.02) µm, where $Z_4 = \lambda\times(6p^4 - 6p^2+1)$ and p is the normalized radius of the pupil [7]. We also know that the wave-front error due to SA is given by the value of the Z_4-coefficient, and a fourth-order Zernike expansion of the peak-to-valley (PV) wave-front gives: $PV = 6\times\sqrt{5}\times Z_4$, thus $PV \sim (3.6 \pm 0.3)$ µm. Since the Seidel sum ${S_I}^C$ and PV are related by the formula ${S_I}^C = 8\times PV$, for a 6-mm aperture diameter we then infer an experimental ${S_I}^C$ value of (0.029 ± 0.002) mm, which is in good agreements (0.026 mm) with our results given in Table 3.

Concerning the stop-shift law, it is also important to note that for a typical value such as $e_1+e_2 = 4.6$ mm, Table 3 shows that the difference between ${S_{II}}^C$ and $({S_{II}}^C)^*$ is around 50% : taking into account the linear pupil shift effect is then mandatory for a good correction of corneal coma.

2.2. IOL aberrations

Using Table 2, the front and back radius of curvature of the IOL can be calculated:

$$R_3 = \frac{2(n_{IOL} - n_2)}{P_{IOL}(X_{IOL} + 1)} \quad \text{and} \quad R_4 = \frac{2(n_{IOL} - n_2)}{P_{IOL}(X_{IOL} - 1)} \tag{7}$$

The conjugate variable Y_{IOL} can also be evaluated using its definition [23] and for our study can be expressed as:

$$Y_{IOL} = 1 + 2\frac{h_1}{h_2}\frac{P_C}{P_{IOL}} \tag{8}$$

As the object and image spaces of the IOL are the same optical media, the expression of the aberrations is, in this case simpler, than for cornea. Taking into account a pure 4^{th}-order aspheric

Biomedical Optics EXPRESS

surface for the anterior and posterior surfaces of the IOL (*i. e.* $\varepsilon_4 \neq 0$), one gets for spherical aberration:

$$S_I^{IOL}(X_{IOL}, \varepsilon_4) = {a_1}^{IOL} X_{IOL}^2 + {a_2}^{IOL} X_{IOL} + {a_3}^{IOL} + {a_4}^{IOL} \varepsilon_4 \tag{9}$$

Where the coefficients of ${S_I}^{IOL}$ are given in Appendix C.

For primary coma of the IOL, formalism of [23] is not enough accurate because the IOL is not totally thin. So, we calculated coma Seidel sums for anterior and posterior surface of the IOL, then used the pupil-shift law that includes extra-coma contribution due to ${S_I}^{IOL}$. After some algebraic manipulations, we found that the primary coma of the IOL is then given by:

$$S_{II}^{IOL}(X_{IOL}, \varepsilon_4) = {b_1}^{IOL} X_{IOL}^2 + {b_2}^{IOL} X_{IOL} + {b_3}^{IOL} + {b_4}^{IOL} \varepsilon_4 \tag{10}$$

Where the corresponding coefficients of ${S_{II}}^{IOL}$, $\{{b_1}^{IOL}, {b_2}^{IOL}, {b_3}^{IOL}\}$ for the spherical part and ${b_4}^{IOL}$ for the aspherical one, are given in Appendix D. It is worth seeing that the proposed Seidel sum for coma given by Eq. (10), is not usual: indeed, we deviate from the classical linear function [5,23] to a quadratic function with X_{IOL}. This advanced quadratic expression enables us to have good results on a wide dioptric range (18 D).

2.3. Pseudophakic eye aberrations and correction

For the whole system, the SA and coma, are given by:

$$S_I^{Tot} = S_I^C + S_I^{IOL}, \; S_{II}^{Tot} = (S_{II}^C)^* + S_{II}^{IOL}. \tag{11}$$

Once the power P_{IOL} of the IOL is provided and the size of the pupil with its field of view are fixed, a first usual approach is the optimization of the overall image quality, by minimizing the RMS-value of the aberrated wavefront, in order to have an aplanatic pseudophakic eye (*i. e.* corrected for on-axis SA and off-axis aberrations). This strategy has already been reported for the design of isoplanatic monofocal IOL [3]. Rather than minimizing this overall RMS-value, we decided to correct each aberration of the pseudophakic eye, by solving the system $\{{S_I}^{Tot} = 0$ and ${S_{II}}^{Tot} = 0\}$ for the variables $\{X_{IOL}$ and $\varepsilon_4\}$, using the shape factor X_{IOL} to optimize off-axis ocular coma and the asphericization ε_4 for the cancellation of SA. Unfortunately, in terms of coma correction, this strategy does not seem to lead to the same solution given when running the iterative optimization of the merit function of Zemax.

We found that the optimal shape factor ${X_{IOL}}^{Opt}$ is determined by solving the following equation:

$$(S_{II}^{Tot} - b_4^{IOL}\varepsilon_4) - \frac{\partial (S_{II}^{Tot} - b_4^{IOL}\varepsilon_4)}{\partial X} u_2' = 0 \tag{12}$$

The merit function, represented by Eq. (12), is the Abbe's Sine Condition for our optical system and is the required condition for an off-axis image free of coma [24]. To our knowledge, this is the first time that such an analytic optimization is proposed. The aspheric coefficient ε_4 has no contribution in this optimization (see Eq. (11) and Eq. (10)). Then, knowing ${X_{IOL}}^{Opt}$, the optimal aspheric coefficient ${\varepsilon_4}^{Opt}$ is easily solved to meet:

$$S_I^{Tot} = 0 \tag{13}$$

Thus, from Eqs. (9–13) the optimal closed-form solution $\{{X_{IOL}}^{Opt}, {\varepsilon_4}^{Opt}\}$, for the shape factor and the asphericization of the IOL that achieve emmetropia, is then remarkably simple and is given by:

$$X_{IOL}^{Opt} = \frac{-({b_2}^{IOL} - 2{b_1}^{IOL} u_2') + \sqrt{({b_2}^{IOL} - 2{b_1}^{IOL} u_2')^2 - 4{b_1}^{IOL}[{b_3}^{IOL} + (S_{II}^C)^* - {b_2}^{IOL} u_2']}}{2{b_1}^{IOL}} \tag{14}$$

Biomedical Optics EXPRESS

and

$$\varepsilon_4^{Opt} = -\frac{a_1{}^{IOL}(X_{IOL}^{Opt})^2 + a_2^{IOL}X_{IOL}^{Opt} + a_3^{IOL} + S_I^C}{a_4^{IOL}} \tag{15}$$

The next section will show that this analytical solution compares very well with results given by ray tracing software Zemax, and that residual oblique astigmatism of the pseudophakic eye is low. Finally, we specify that due to the natural radius of curvature of the retina and its negative sign (see Table 1), we don't need to cancel the field curvature of the whole system, and as the pseudophakic eye has only positive lenses (cornea and IOL), its Petzval curvature is also always negative.

3. Results

3.1. Examples of personalized design and performance

In order to verify the proposed analytical model, we design the IOL that corrects the LBME model for cornea (Table 1), arbitrarily supposing a 4.5 mm-diameter incident rays ($h_1 = 2.25$ mm), an ocular kappa angle $\kappa_1 = 5.5°$, $n_{IOL} = 1.46$, $e_{IOL} = 1.1$ mm, $P_{IOL} = 22$ D and $e_2 = 4.1$ mm. For all the considered IOLs, it is possible to take as a good approximation $h_3 \sim 0.95{\times}h_2$. Using Tables (2, 3), Eqs. (16–33), and Eqs. (14, 15), one can find that the optimal IOL is given by: ${X_{IOL}}^{Opt} = -0.1977$ and ${\varepsilon_4}^{Opt} = -0.00063$. Front and back radius of curvature of this IOL are

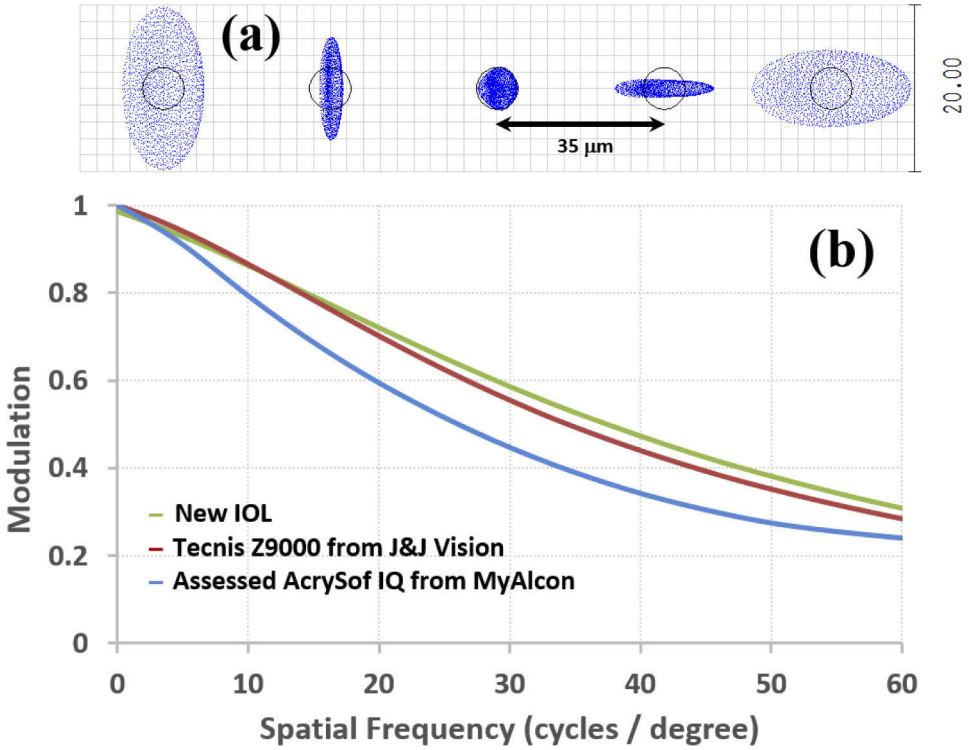

Fig. 2. Pseudophakic eye with the new IOL and calculated for 4.5 mm ocular pupil diameter. (a) Through focus spot diagram on retina for a delta focus of 35 µm. Radius of Airy disk (black) is 2.5 µm and aberrated RMS radius of spot diagram (blue) is 1.7 µm. (b) MTF plots of the pseudophakic eye with the new IOL, Tecnis Z9000 and Assessed AcrySof IQ. The power of these IOLs is 22 D, $\lambda = 555$ nm, $e_2 = 4.1$ mm and ocular kappa angle $\kappa_1 = 5.5°$.

Biomedical Optics EXPRESS

then calculated using Eq. (7): $R_3 = 14.06$ mm and $R_4 = -9.41$ mm. The optical performances of this design are very good and shown in Fig. 2. With the calculated new IOL, the pseudophakic eye is diffraction limited as shown in the spot diagrams in Fig. 2(a) and the resolution given by the modulation transfer function (MTF) in Fig. 2(b). For comparison, Fig. 2(b) also shows MTF plots of the commercial Tecnis Z9000 IOL supplied by J&J Vision (AMO) and AcrySof IQ from MyAlcon. The datas for the Tecnis Z9000 IOL and AcrySof IQ, respectively taken from [8] and [25], show that the form of those IOLs are very complex including conic constant, 4th- and 6th-high order of aspheric terms. The Tecnis Z9000 IOL was designed to compensate an average RMS corneal SA of + 0.27 mm at 6 mm pupil. Table 3 and calculation below this table show that this value is very close to the corneal SA of the LBME cornea model, that can be then approximated as a cornea model for the Tecnis Z9000 design. Concerning AcrySof IQ, no aspheric surface specifications of this IOL was found in the literature and the approximation was introduced based on the reference that AcrySof IQ manifested about 74% of spherical aberration of the Tecnis Z9000 (0.74×0.27 = 0.2 mm) [25]. Thus, we modified the conic constant of the anterior cornea of the LBME model (from -0.18 to -0.282) to have a corresponding cornea model for AcrySof IQ design. The corresponding IOL was referred to as "Assessed AcrySof IQ". Figure 2 shows that the new proposed IOL has similar optical performances than those obtained with the Tecnis Z9000. We recall that this new IOL design has neither conic constant nor 6th-aspheric term.

For the pseudophakic eye with the new IOL of power 22 D, Table 4 shows the Seidel sums calculated with the proposed formalism and compared with the iterative spot diagram optimization process given by Zemax, demonstrating the validity of the proposed analytical model.

Table 4. Aberrations of the pseudophakic eye with the new IOL of power 22 D

	$S_I{}^C$	$S_I{}^{IOL}$	$(S_{II}{}^C)*$	$S_{II}{}^{IOL}$
Calculated with the model proposed in this paper	0.0082	−0.0082	0.0019	−0.002
Calculated with Zemax	0.0081	−0.0083	0.00189	−0.002

Table 4 and Table 2 also show that the whole pseudophakic eye is aplanatic, indeed: size of sagittal coma is $S_{II}{}^{Tot}/(2n_2u'_2) \sim 0.5$ µm and Zemax gives us a longitudinal astigmatism $S_{III}{}^{Tot}/(n_2 u'^2_2) \sim 40$ µm (<0.13 D). Moreover, the pseudophakic eye remains diffraction-limited for field

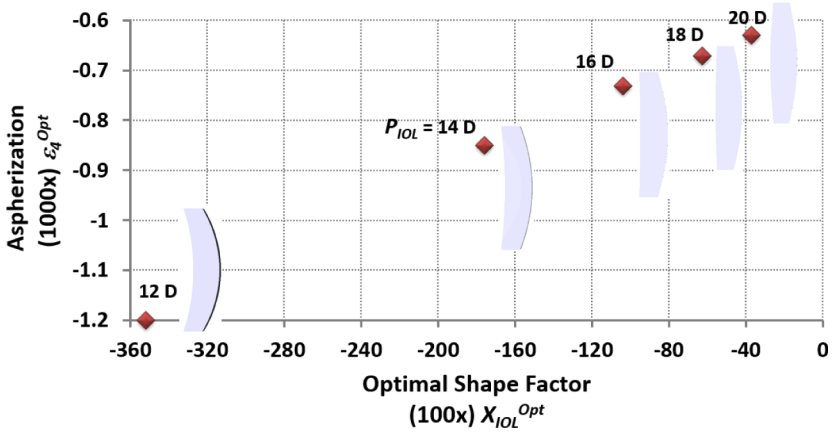

Fig. 3. Optimized lenses for LBME cornea: 4th-order aspherization as a function of optimal shape for power ranging from 12 to 20 D (pupil diameter: 4.5 mm). For all those IOLs the pseudophakic eyes are diffraction-limited.

Biomedical Optics EXPRESS

angles ranging from [κ_1-12°, κ_1+1°] around the Y direction and ± 2.5° around the X axis (see Fig. 1 for axis convention).

As a second application, setting the required power of the lens as a parameter, we calculated the best IOLs for biometric LBME model of cornea, ocular kappa angle $\kappa_1 = 5.5°$, 4.5 mm pupil diameter, $n_{IOL} = 1.46$, $e_{IOL} = 1.1$ mm and $e_2 = 4.1$ mm. For power ranging from 12 D to 30 D, optimized profiles $\{X_{IOL}{}^{Opt}, \varepsilon_4{}^{Opt}\}$ of the new lens are reported in Figs. 3 and 4. Note that with all presented IOLs, the pseudophakic eyes are diffraction limited.

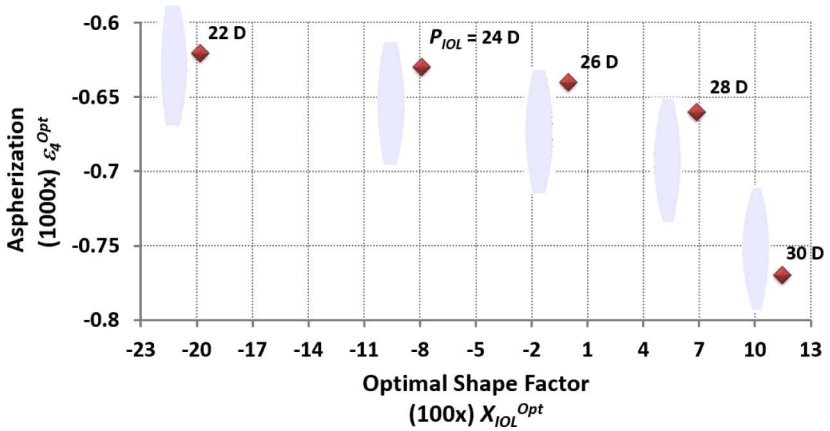

Fig. 4. Optimized lenses for LBME cornea: 4th-order aspherization as a function of optimal shape for power ranging from 22 to 30 D (pupil diameter: 4.5 mm). For all those IOLs the pseudophakic eyes are diffraction-limited.

For power ranging from 12 D to 30 D, Tables 5 and 6 show a good correlation between the analytic solution with the predictions given by Zemax.

Table 5. Analytic solution versus Zemax result for the shape factor *X*

P_{IOL}	12	14	16	18	20 D	22	24	26	28	30
$X_{IOL}{}^{Opt}$ (model)	−3.53	−1.76	−1.04	−0.63	−0.37	−0.198	−0.079	0	0.069	0.114
X_{IOL} (Zemax)	−3.49	−1.67	−1.08	−0.64	−0.38	−0.219	−0.089	0	0.059	0.103

Table 6. Analytic solution versus Zemax result for the aspherization ε_4

P_{IOL}	12	14	16	18	20D	22	24	26	28	30
ε_4 ($\times 10^5$) (model)	−120	−85	−73	−67	−63	−63	−63	−64	−66	−70
ε_4 ($\times 10^5$) (Zemax)	−123	−78	−73	−66	−64	−63	−63	−64	−67	−71

Finally, Fig. 5 shows optical performance of the pseudophakic eye with the new lens, for the two extreme values $P_{IOL} = 12$ D and $P_{IOL} = 30$ D

3.2. Sensitivity to decentration and tilt

The impact of decentration and tilt of the new IOL on the optical performances is evaluated with Zemax simulation (see Fig. 1 for axis convention) for power ranging from 12 D to 30 D, and also compared with those given by Tecnis Z9000 and Assessed AcrySof IQ. For a 4.5 mm ocular pupil diameter, Fig. 6 shows the convolution of the eye's point spread function with the E Snellen optotype for the former IOLs of 22 D, and for decentration and tilt angle of respectively ± 0.3 mm and ± 3°.

Biomedical Optics EXPRESS

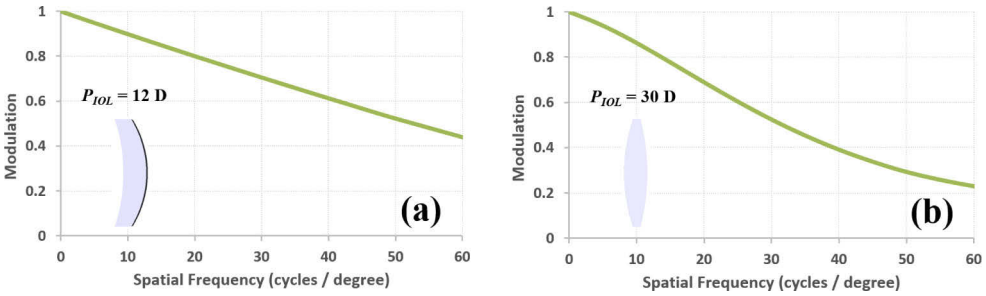

Fig. 5. MTF plots of the pseudophakic eye with the new IOL (pupil diameter: 4.5 mm, $e_2 = 4.1$ mm and kappa angle $\kappa_1 = 5.5°$). (a) $P_{IOL} = 12$ D and (b) $P_{IOL} = 30$ D.

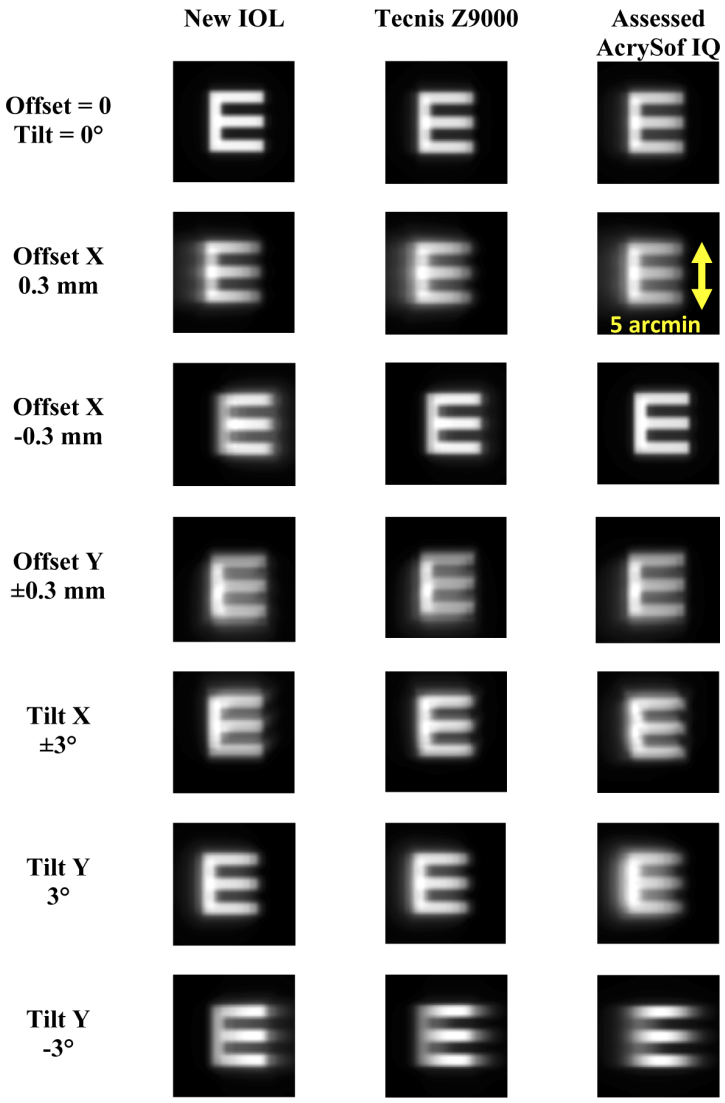

Fig. 6. Effects of decentration and tilt on the convolution of the eye's point spread function with the E Snellen letter. For all IOLs: pupil diameter is 4.5 mm and dioptric power is 22 D. See Fig. 1 for axis convention.

Biomedical Optics EXPRESS

The new aspheric IOL and the Tecnis Z9000 IOL have the same sensitivity to decentration and tilt.

3.3. Sensitivity to postoperative IOL position (e_2)

It is known that the main problem of IOL power calculation is the prediction of the IOL position after surgery (postoperative aqueous depth AD) that contributes to the greatest proportion of IOL power refractive errors. The postoperative AD that is included in well-known, third-generation IOL power calculation formulas SRK/T [26], Holladay 1 [27], and Hoffer Q [28], does not reflect the true postoperative AD in the anatomical sense, because it is calculated using thin lens formulas. Newer formulas require additional biometry parameters, especially those related to anterior segment anatomy, to better predict the postoperative AD [29,30]. With the use of a regression formula, Olsen showed that the postoperative AD could be predicted with an accuracy of ± 0.22 mm [29], whereas very recent works showed that the postoperative IOL position can be accurately predicted using preoperative AD as sole predictor [31]. In this former Reference, the accuracy of the prediction of the postoperative IOL position is ± 0.17 mm. For aberrations correction, the effective IOL position (postoperative AD) is not a parameter as crucial as for IOL power calculation. Indeed, Eq. (6) and Table 3 show that a variation $\delta e_2 = \pm 0.3$ mm lead to a difference in the evaluation of coma of only 6%.

4. Validity of the model

4.1. Performances of the new IOL in the ISO and Physiologic Model Eye

The international standard for evaluation of imaging quality of IOL prescribes a model eye with an essentially aberration-free artificial cornea. The metric by which the lens is evaluated is the modulation at 100 cycles / mm. For acceptable manufacturing, the requirement is that this value be 0.43 or higher for a 3-mm aperture at the IOL using monochromatic light close to 546 nm (ISO 11979-2). In practice, the aberration-free cornea is achieved with available achromat doublets. A possible realization of the model eye of the ISO standard was proposed by Norrby [32] and is shown in Table 7. For IOLs with negative SA, designed to counter the positive SA of the cornea, lower modulation in the ISO model can no longer be interpreted as lower quality for the patient. Thus, a model eye with a physiologic level of SA in the artificial cornea was also proposed by Norrby *et al.* [33]. This last model, represented in Table 8, has dimensions close to the natural eye and is called the Physiological Eye Model.

Table 7. Model Eye of the ISO standard for evaluation of IOL (from [32])

Surface	Radius (mm)	Thickness (mm)	Conic constant	Material / optical index
1	24.59	5.21	0	SSK4
2	−15.58	1.72	0	SF8
3	−90.2	3	0	n = 1
Window front	Flat	6	-	BK7
Window back	Flat	6.25	-	n = 1.336
Iris pupil	Flat	10	-	n = 1.336
Window front	Flat	6	-	BK7
Window back	Flat	9.25	-	1
Image				

Figure 7 illustrates how the new proposed IOLs (calculated to correct the LBME model for cornea) perform in these two former model eyes. For this simulation, an aperture stop of 3 mm was used in direct contact (iris pupil plane) with the anterior surface of the IOL, and following

Biomedical Optics EXPRESS

Table 8. Physiological Model Eye for evaluation of IOL (from [33])

Surface	Radius (mm)	Thickness (mm)	Conic constant	Material / optical index
Anterior Cornea	7.8	0.5	–0.0205	n = 1.496
Posterior Cornea	7.02	4	0	n = 1.336
Iris pupil	Flat	10	-	n = 1.336
Window front	Flat	1	-	BK7
Window back	Flat	16.65	-	n = 1
Image				

the calculations of [32], defocusing was performed to obtain the maximum on-axis MTF at 100 cycles / mm as prescribed. Figure 7 shows that all the new IOLs are well above the approval manufacturing limit of 0.43 modulation at 100 cycles / mm for monochromatic light (546 nm) with a 3 mm iris pupil in the ISO Model Eye and in the Physiological Model Eye. For the particular case of the new IOL of dioptric power 22 D, this value is 0.65.

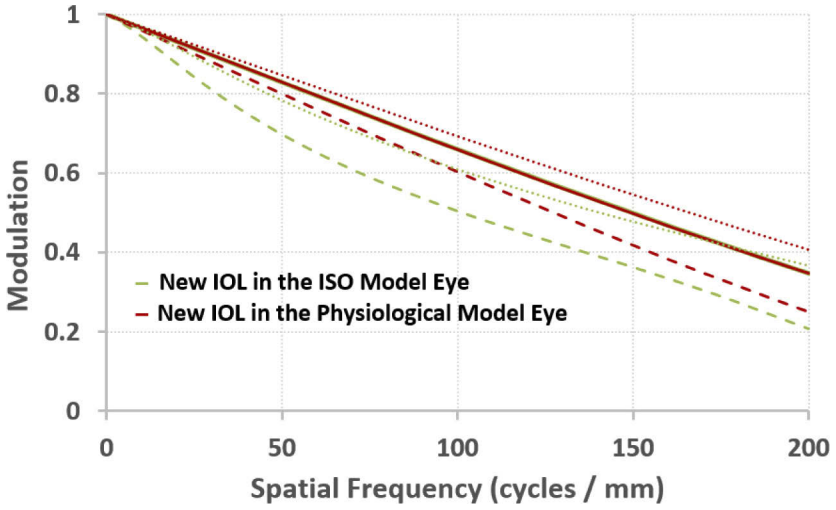

Fig. 7. Calculated MTF curves of the new IOLs in the ISO Model Eye (Green) and Physiological Model Eye (Red). Solid line: 22 D, dash: 12 D, dots: 30 D. Pupil diameter: 3 mm, $\lambda = 546$ nm and $\kappa_1 = 0°$.

4.2. Limitations of the proposed model

Usually, the design of commercial aberration-correcting IOLs is complex, generally including conic constant, 4^{th}- and 6^{th}- power of aspheric terms [8,11,17]. The proposed analytical model only considers 4^{th}-order aspheric term in the new IOL. This imply that it is not possible to find an optimized aberration-correcting lens for all the ocular biometry of each patient. Mathematically speaking, the model fails to design the shape of the IOL if the expression under the square root sign of Eq. (14) is negative. When it is the case, it means that it is not possible to just use the Coddington factor and one aspheric value, for perfect aberration correction. Another way to visualize this comes from Eq. (2). Indeed, we saw with this equation that the values Q' and ε_4 can be interchanged and generally, the use of the asphericization term ε_4 is more efficient than Q' for aberration compensation [3]. However, Eq. (2) is also invalid when the surface radius R ($=1/c_u$) is too small such that the term $(1\text{-}c_u^2h^2)^{1/2}$ becomes a complex number. When this happens, the model fails to design the shape of the IOL.

Biomedical Optics EXPRESS

Main parameters of influence are n_{IOL}, e_2, P_{IOL} and Fig. 8 illustrates the validity of the analytic model for the LBME model of cornea. For example, if we suppose an IOL with optical refractive index 1.49, set-up at a distance e_2=3.5 mm, it is possible to design aberration-correcting lenses with dioptric power ≥ 13 D, whereas lenses with dioptric power < 13 D are not possible for a perfect coma correction of the pseudophakic eye (see Fig. 8 c)). If the total ocular Seidel coma aberration cannot be zero because corneal power, postoperative chamber length and optical index of the IOL do not satisfy Eq. (14), it can be minimized ($(S_{II}{}^{Tot})_{min}$). The value $X_{IOL}{}^{Min}$ of the bending factor minimizing the total coma aberration and the corresponding minimum coma aberration are then given by :

$$X_{IOL}^{Min} = \frac{-b_2{}^{IOL}}{2b_1{}^{IOL}} + u'_2 \quad \text{and} \quad (S_{II}^{Tot})_{Min} = S_{II}^{Tot}(X_{IOL}^{Min}, \varepsilon_4) \tag{16}$$

Finally, Fig. 8 also shows that for eyes with short postoperative internal anterior chamber (2.5 mm < e_2 < 3 mm), the design of an IOL with a low dioptric power (for example $P_{IOL} \leq 13.5$ D), is only possible with the proposed model, if the optical index of the IOL is low.

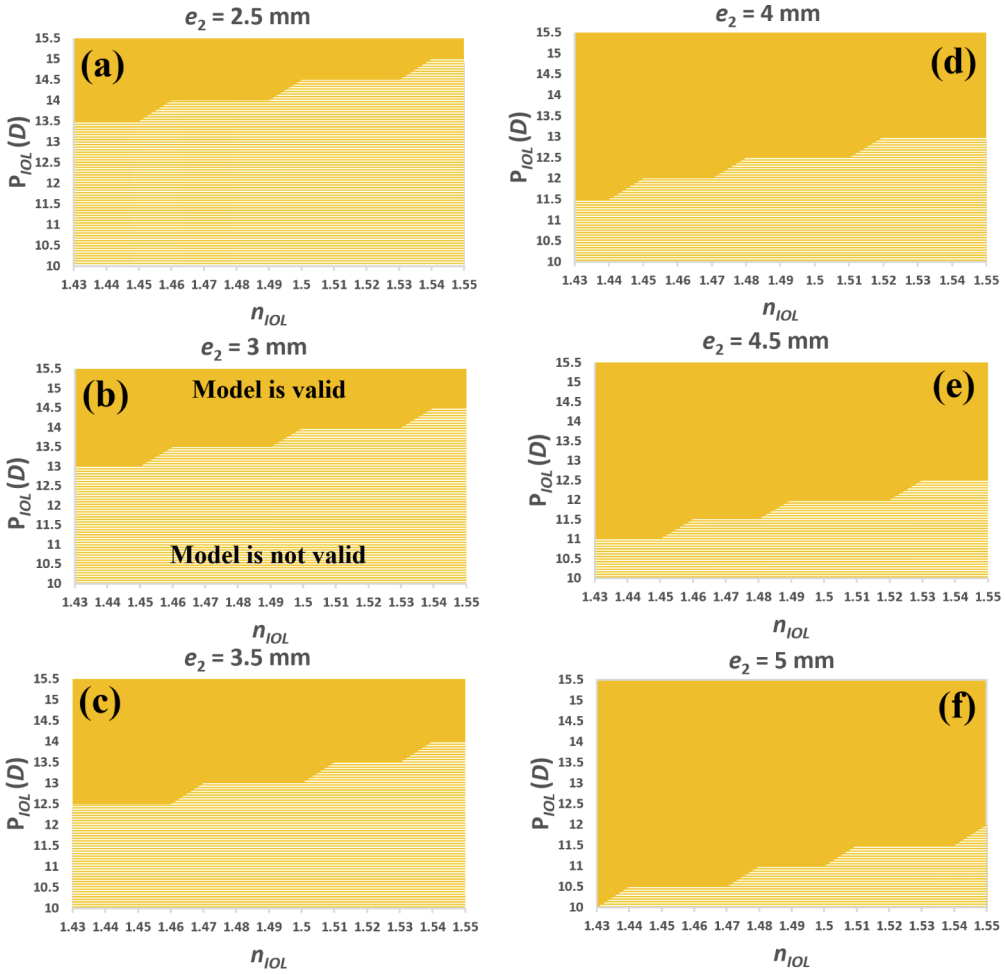

Fig. 8. Validity of the calculation of the new IOL for a total correction of coma of the LBME model of cornea, as a function of n_{IOL} and P_{IOL}, for $e_2 = 2.5$ mm (a) to $e_2 = 5$ mm (f). Pupil: 4.5 mm, Kappa angle $\kappa_1 = 5.5°$.

Biomedical Optics EXPRESS

5. Conclusions

We have derived an analytical formulation determining the required shape for a new aspheric IOL able to minimize global on- and off-axis aberrations of a pseudophakic eye. This proposed calculating tool, within the framework of the Seidel theory of third-order optical aberrations, takes into account for the first time to our knowledge, corneal conicities, 4^{th}-order aspheric surface, pupil-shift effect and ocular kappa angle, enables personalized IOL design. Part of the optimization is realized considering a "pure" 4^{th}-order aspheric term (no conic term) for the surfaces of the new IOL in order to minimize SA, whereas we used the Abbe's Sine Condition to minimize off-axis aberration (coma) of the pseudophakic eye.

Moreover, we show in this paper that the use of such geometrical surfaces for the IOL enables pure analytical solution for the optimized pseudophakic eye. This can be of great interest for researchers or designers.

Concerning the manufacturing process of those personalized IOL designs, molding lenses approach can be very time-consuming and expensive because we are aiming to make customized IOLs and only a few units per patient are required. Therefore, milling process, high precision lathe cutting, or additive manufacturing would be interesting alternatives. Concerning this former 3-D printing process, the limits of this technology come down to what materials are available and the resolution at which current machines can print. New materials (able to withstand the 3-D printing process while maintaining its clarity, shape and size) have to be developed and then approved for medical purposes (FDA approval process for example). We note that an attempt of three-dimensional printing of the historical Ridley lens was made, but the overall optical quality of the printed lens (surface roughness, etc..) was far from clinical standards and needs to be improved [34].

As soon as the biometry of the cornea is known and once the power of the IOL has been determined by the ophthalmologist, all the cascading formulas on this manuscript can be calculated using a simple Microsoft Excel sheet (see supplementary information at the end of this paper), up to Eq. (14) and Eq. (15) of the optimal personalized IOL that achieve emmetropia for the pseudophakic eye. For IOL power ranging from 12 D to 30 D this analytical solution compares very well with results given by the iterative optimization process of the merit function of Zemax.

In terms of retinal optical quality, we also showed that the new proposed 4^{th}-order aspheric IOL compares well (MTF, decentration / tilt sensitivities) with commercial Tecnis Z9000 IOL supplied by Johnson & Johnson Vision, whose design is much more complex (conic constant + 4^{th}- + 6^{th}-order of aspheric terms). We believe that this new aberration-correcting IOL has the potential to offer a route to the manufacturing of personalized intraocular lens.

6. Supplemental document

A calculating tool as we show in Code 1 (Ref. [35]) enables the design for a personalized aberration-correcting IOL, as a function of the cornea's parameters.

Appendix A: Numerical values for SA's corneal coefficients (from [23])

$a_1{}^C$	$a_2{}^C$	$a_3{}^C$	$a_4{}^C$	$a_5{}^C$	$a_6{}^C$	$a_7{}^C$	$a_8{}^C$	$a_9{}^C$	$a_{10}{}^C$
−585.455	−0.44	64.943	0.365	1856.017	7.222	−165.894	−1885.886	62.892	676.378

Appendix B: Numerical values for coma's corneal coefficients (from [23])

Biomedical Optics EXPRESS

$p_1{}^C$	$p_2{}^C$	$p_3{}^C$	$p_4{}^C$	$p_5{}^C$	$p_6{}^C$
−16.236	0.44	−0.183	41.473	−4.391	−15.613

Appendix C: Parameters for spherical aberration of the IOL

Coefficient a_4^{IOL} represents the aspherical part of SA and the spherical coefficients $\{ a_1{}^{IOL}, a_2{}^{IOL}, a_3{}^{IOL}\}$ are calculated from [23].

$$a_1^{IOL} = \frac{1}{4}h_{mean}^4 P_{IOL}^3 \frac{n_{IOL} + 2n_2}{n_{IOL}(n_{IOL} - n_2)^2} \tag{17}$$

$$a_2^{IOL} = -\frac{1}{4}h_{mean}^4 P_{IOL}^3 \frac{4(n_{IOL} + n_2)}{n_{IOL}n_2(n_{IOL} - n_2)} Y_{IOL} \tag{18}$$

$$a_3^{IOL} = \frac{1}{4}h_{mean}^4 P_{IOL}^3 [\frac{3n_{IOL} + 2n_2}{n_{IOL}n_2^2} Y_{IOL}^2 + \frac{n_{IOL}^2}{n_2^2(n_{IOL} - n_2)^2}] \tag{19}$$

$$a_4^{IOL} = 8(n_{IOL} - n_2)h_2^4 - 8(n_2 - n_{IOL})h_3^4 \tag{20}$$

Appendix D: Parameters for coma of the IOL

Coma Seidel sums are calculated for anterior and posterior surface of the IOL considered here as a thin lens. Then, the pupil-shift law including extra-coma contribution due to $S_I{}^{IOL}$ is used, to find the quadratic expression of $S_{II}{}^{IOL}$. It is easy to show that if $e_{IOL} = 0$ and $h_2 = h_3$ (thin lens approximation) then $b_1{}^{IOL} = 0$.

$$\chi = \frac{e_{IOL}\kappa_1}{n_{IOL}h_3} \tag{21}$$

$$A_1 = \frac{1}{2}n_2 h_2 H P_{IOL}^2 \tag{22}$$

$$A_2 = A_1 \frac{h_2}{2n_{IOL}^2(n_{IOL} - n_2)} \tag{23}$$

$$A_3 = A_1 \frac{h_1 P_C}{(n_{IOL} - n_2)P_{IOL}}(\frac{1}{n_{IOL}^2} - \frac{1}{n_2^2}) + A_2 \left[1 + \frac{n_{IOL}}{n_2} + Y_{IOL}(1 - \frac{n_{IOL}}{n_2})\right] \tag{24}$$

$$A_4 = A_1(\frac{n_{IOL}}{n_2(n_{IOL} - n_2)} - \frac{Y_{IOL}}{n_2}) \left[\frac{h_2}{2n_{IOL}^2} + \frac{h_1 P_C}{P_{IOL}}(\frac{1}{n_{IOL}^2} - \frac{1}{n_2^2})\right] \tag{25}$$

$$A_5 = \frac{1}{2}n_2 h_3 H P_{IOL} \tag{26}$$

$$A_6 = \frac{n_{IOL}}{n_2^2} - \frac{1}{n_{IOL}} \tag{27}$$

$$A_7 = \frac{A_5 P_{IOL}}{(n_{IOL} - n_2)} \left[\frac{A_6 h_2}{2n_{IOL}} - \frac{h_3}{2n_2^2}\right] \tag{28}$$

$$A_8 = \frac{h_3 P_{IOL}}{2n_2^2} + A_6(\frac{h_2 P_{IOL}}{2n_{IOL}} + \frac{h_1 P_C}{n_{IOL}}) \tag{29}$$

$$A_9 = \frac{A_5 A_8}{(n_{IOL} - n_2)} - \frac{A_7(n_{IOL} - n_2)}{n_2}[Y_{IOL} + \frac{n_{IOL}}{(n_{IOL} - n_2)}] \tag{30}$$

Biomedical Optics EXPRESS

$$A_{10} = \frac{-A_5 A_8}{n_2}\left[Y_{IOL} + \frac{n_{IOL}}{(n_{IOL} - n_2)}\right] \tag{31}$$

$$b_1^{IOL} = A_2 + A_7 + \chi a_1^{IOL} \tag{32}$$

$$b_2^{IOL} = A_3 + A_9 + \chi a_2^{IOL} \tag{33}$$

$$b_3^{IOL} = A_4 + A_{10} + \chi a_3^{IOL} \tag{34}$$

$$b_4^{IOL} = 8(n_2 - n_{IOL})h_3^4\chi \tag{35}$$

Funding

Agence Nationale de la Recherche (LAPHIA ANR - n°ANR- 10-IDEX-03-02).

Acknowledgments

We thank Pr. David Touboul (CHU, Bordeaux in FRANCE) for discussions on IOLs and our two anonymous Reviewers for advices and the constructive revision of this manuscript.

Disclosures

The authors declare that there are no conflicts of interest related to this article.

References

1. C. Canovas and P. Artal, "Customized eye models for determining optimized intraocular lenses power," Biomed. Opt. Express **2**(6), 1649–1663 (2011).
2. J. X. Kane, A. Van Heerden, A. Atik, and C. Petsoglou, "Intraocular lens power formula accuracy: comparison of 7 formulas," J. Cataract Refractive Surg. **42**(10), 1490–1500 (2016).
3. S. Barbero, S. Marcos, J. Montejo, and C. Dorronsoro, "Design of isoplanatic aspheric monofocal intraocular lenses," Opt. Express **19**(7), 6215–6230 (2011).
4. G. Smith and C. W. Lu, "The spherical aberration of intra-ocular lenses," Oph. Phys. Optics **8**, 287–294 (1988).
5. C. Chen, "Methods of solving aspheric singlets and cemented doublets with given primary aberrations," Appl. Opt. **53**(29), H202–H212 (2014).
6. D. A. Atchison, "Design of aspheric intraocular lenses," Oph. Phys. Optics **11**, 137–146 (1991).
7. J. T. Holladay, P. A. Piers, G. Koranyi, M. Van der Mooren, and N. E. S. Norrby, "A new intraocular lens design to reduce spherical aberration of a pseudophakic eye," J. Refract. Surg. **18**, 683–691 (2002).
8. S. Norrby, P. Artal, P. A. Piers, and M. Van der Mooren, "Methods of obtaining ophthalmic lenses providing the eye with reduced aberrations," US Patent 6,609,793.
9. M. Gerlach and C. Lesage, "Aspheric intraocular lens and method for designing such IOL" WO Patent 2007/128423.
10. G. E. Altmann, L. D. Nichamin, S. S. Lane, and J. S. Pepose, "Optical performance of 3 intraocular lens designs in the presence of decentration," J. Cataract Refractive Surg. **31**(3), 574–585 (2005).
11. T. Eppig, K. Scholz, A. Löffler, A. Mesner, and A. Langenbucher, "Effect of decentration and tilt on the image quality of aspheric intraocular lens design in a model eye," J. Cataract Refractive Surg. **35**(6), 1091–1100 (2009).
12. R. Bellucci, S. Morselli, and V. Pucci, "Spherical aberration and coma with aspherical and a spherical intraocular lens in normal age-matched eyes," J. Cataract Refractive Surg. **33**(2), 203–209 (2007).
13. T. D. Sauer, "Tilt and decentration of intraocular lenses – a brief review," Adv. Ophthalmol. Vis. Syst. **2**(4), 115–117 (2015).
14. A. de Castro, P. Rosales, and S. Marcos, "Tilt and decentration of intraocular lenses in vivo Purkinje and Scheimpflug imaging – Validation study," J. Cataract Refractive Surg. **33**(3), 418–429 (2007).
15. J. Tabernero, P. Piers, A. Benito, M. Redondo, and P. Artal, "Predicting the optical performance of eyes implanted with IOLs to correct spherical aberration," Invest. Ophthalmol. Visual Sci. **47**(10), 4651–4658 (2006).
16. F. Taketani, E. Yukawa, T. Yoshii, Y. Sugie, and Y. Hara, "Influence of intraocular lens optical design on high-orders aberrations," J. Cataract Refractive Surg. **31**(5), 969–972 (2005).
17. J. Tabernero, P. Piers, and P. Artal, "Intraocular lens to correct corneal coma," Opt. Lett. **32**(4), 406–408 (2007).
18. G. Smith and C. W. Lu, "Peripheral power errors and astigmatism of eyes corrected with intraocular lenses," Optom. Vis. Sci. **68**(1), 12–21 (1991).
19. http://www.zemax.com
20. S. Marcos, P. Rosales, L. Llorente, S. Barbero, and I. Jiménez-Alfaro, "Balance of corneal horizontal coma by internal optics in eyes with intraocular artificial lenses: Evidence of a passive mechanism," Vision Res. **48**(1), 70–79 (2008).
21. S. Barbero and S. Marcos, "Analytical tools for customized design of monofocal intraocular lenses," Opt. Express **15**(14), 8576–8591 (2007).

Biomedical Optics EXPRESS

22. H. L. Liou and N. A. Brennan, "Anatomically accurate, finite model eye for optical modelling," J. Opt. Soc. Am. A **14**(8), 1684–1695 (1997).
23. L. N. Hazra and C. A. Delisle, "Primary aberrations of a thin lens with different object and image space media," J. Opt. Soc. Am. A **15**(4), 945–953 (1998).
24. M. Born and E. Wolf, *Principle of Optics*, 6th ed. Pergamon Press, Oxford, U. K. (1980).
25. V. Portney, "New bi-sign aspheric IOL and its application," Optom. Vis. Sci. **89**(1), 80–89 (2012).
26. J. A. Retzlaff, D. R. Sanders, and M. C. Kraff, "Development of the SRK/T intraocular lens implant power calculation formula," J. Cataract Refractive Surg. **16**(3), 333–340 (1990).
27. J. T. Holladay, T. C. Prager, T. Y. Chandler, K. H. Musgrove, J. W. Lewis, and R. S. Ruiz, "A three-part system for refining intraocular lens power calculations," J. Cataract Refractive Surg. **14**(1), 17–24 (1988).
28. K. J. Hoffer, "The Hoffer Q formula: a comparison of theoretic and regression formulas," J. Cataract Refractive Surg. **19**(6), 700–712 (1993).
29. T. Olsen, "Prediction of intraocular lens position after cataract extraction," J. Cataract Refractive Surg. **12**(4), 376–379 (1986).
30. T. Olsen, "Prediction of the effective postoperative (intraocular lens) anterior chamber depth," J. Cataract Refractive Surg. **32**(3), 419–424 (2006).
31. S. Norrby, R. Bergman, N. Hirnschall, Y. Nishi, and O. Findl, "Prediction of the true IOL position," Br. J. Ophthalmol. **101**(10), 1440–1446 (2017).
32. S. Norrby, "Standardized methods for assessing the imaging quality of intraocular lenses," Appl. Opt. **34**(31), 7327–7333 (1995).
33. S. Norrby, P. Piers, C. Campbell, and M. Van der Mooren, "Model eyes for evaluation of intraocular lenses," Appl. Opt. **46**(26), 6595–6605 (2007).
34. G. Debellemanière, M. Flores, M. Montard, B. Delbosc, and M. Saleh, "Three-dimensional printing of optical lenses and ophthalmic surgery: challenges and perspectives," J. Refract. Surg. **32**(3), 201–204 (2016).
35. B. Chassagne and L. Canioni, "Microsoft Excel sheet for aberration-correcting IOL design" figshare, https://doi.org/10.6084/m9.figshare.10093412 (2019).